

Far UV-C radiation: An emerging tool for pandemic control

Ernest R. Blatchley III, David J. Brenner, Holger Claus, Troy E. Cowan, Karl G. Linden, Yijing Liu, Ted Mao, Sung-Jin Park, Patrick J. Piper, Richard M. Simons & David H. Sliney

To cite this article: Ernest R. Blatchley III, David J. Brenner, Holger Claus, Troy E. Cowan, Karl G. Linden, Yijing Liu, Ted Mao, Sung-Jin Park, Patrick J. Piper, Richard M. Simons & David H. Sliney (2022): Far UV-C radiation: An emerging tool for pandemic control, *Critical Reviews in Environmental Science and Technology*, DOI: [10.1080/10643389.2022.2084315](https://doi.org/10.1080/10643389.2022.2084315)

To link to this article: <https://doi.org/10.1080/10643389.2022.2084315>



© 2022 The Author(s). Published with license by Taylor & Francis Group, LLC.



[View supplementary material](#)



Published online: 10 Jun 2022.




[Submit your article to this journal](#)



[View related articles](#)

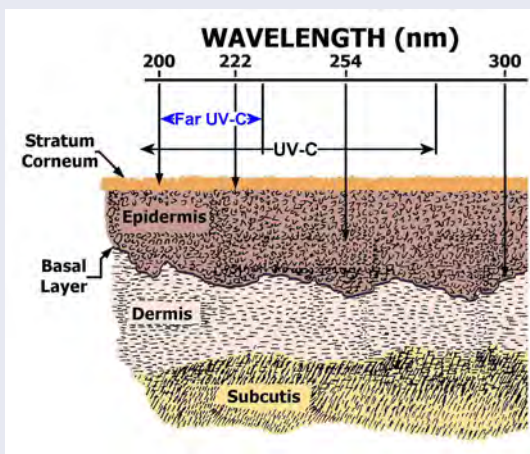
Far UV-C radiation: An emerging tool for pandemic control

Ernest R. Blatchley III^a , David J. Brenner^b, Holger Claus^c, Troy E. Cowan^d, Karl G. Linden^e, Yijing Liu^f, Ted Mao^g, Sung-Jin Park^h, Patrick J. Piperⁱ, Richard M. Simons^j, and David H. Sliney^k

^aLyles School of Civil Engineering and Division of Environmental and Ecological Engineering, Purdue University, West Lafayette, Indiana, USA; ^bCenter for Radiological Research, Columbia University Irving Medical Center, New York, New York, USA; ^cUshio America, Inc., Cypress, California, USA; ^dVision Based Consulting, LLC, Lexington Park, Maryland, USA; ^eDepartment of Civil, Environmental, and Architectural Engineering, University of Colorado, Boulder, Colorado, USA; ^fDepartment of Civil, Environmental and Geodetic Engineering, Ohio State University, Columbus, Ohio, USA; ^gMW Technologies, Inc., London, Canada; ^hEden Park Illumination, Inc., Champaign, Illinois, USA; ⁱFar UV Technologies, Kansas City, Missouri, USA; ^jAquiSense Technologies, Erlanger, Kentucky, USA; ^kBloomberg School of Public Health, Johns Hopkins University, Baltimore, Maryland, USA

ABSTRACT

Far UV-C, informally defined as electromagnetic radiation with wavelengths between 200 and 230 nm, has characteristics that are well-suited to control of airborne pathogens. Specifically, Far UV-C has been shown to be highly effective for inactivation of airborne pathogens; yet this same radiation has minimal potential to cause damage to human skin and eye tissues. Critically, unlike UV-B, Far UV-C radiation does not substantially penetrate the dead cell layer of skin (stratum corneum) and does not reach germinative cells in the basal layer. Similarly, Far UV-C radiation does not substantially penetrate through corneal epithelium of the eye, thereby preventing exposure of germinative cells within the eye. The most common source of Far UV-C radiation is the krypton chloride excimer (KrCl^*) lamp, which has a primary emission centered at 222 nm. Ozone production from KrCl^* lamps is modest, such that control of indoor ozone from these systems can be accomplished easily using conventional ventilation systems. This set of characteristics offers the potential for Far UV-C devices to be used in occupied spaces, thereby allowing for improved effectiveness for inactivation of airborne pathogens, including those that are responsible for COVID-19.



KEYWORDS Air disinfection; Coronavirus; disinfection; Far UV-C; ozone; safety

HANDLING EDITORS Taicheng An and Scott Bradford

CONTACT Ernest R. Blatchley III  blatch@purdue.edu  Lyles School of Civil Engineering and Division of Environmental and Ecological Engineering, Purdue University, West Lafayette, IN, USA.

 Supplemental data for this article is available online at <https://doi.org/10.1080/10643389.2022.2084315>.

© 2022 The Author(s). Published with license by Taylor & Francis Group, LLC.

This is an Open Access article distributed under the terms of the Creative Commons Attribution-NonCommercial License (<http://creativecommons.org/licenses/by-nc/4.0/>), which permits unrestricted non-commercial use, distribution, and reproduction in any medium, provided the original work is properly cited.

Introduction

Beginning as early as the 1930s, UV-C radiation (100–280 nm) has been applied for disinfection of air and surfaces (Wells & Fair, 1935; Reed, 2010). Since that time, UV-C-based disinfection systems have been demonstrated to be effective for reduction of disease transmission, even for highly contagious viral diseases, such as measles, influenza, and the common cold.

Conventional UV-C applications have been based on low-pressure mercury lamps, which are characterized by a primary emission line at 253.7 nm. UV-C radiation at this wavelength causes inactivation of pathogens *via* damage to nucleic acids (DNA and RNA). However, this same radiation is known to cause damage to mammalian skin and eyes. Consequently, conventional UV-C systems for disinfection of air and surfaces must be designed and operated in a manner that minimizes exposure of human tissues.

Recent research has demonstrated that Far UV-C radiation (200–230 nm) has minimal potential to damage mammalian skin and eye tissues. Yet, Far UV-C radiation tends to be at least as effective as conventional UV-C radiation for inactivation of most microbial and viral pathogens, including those that are responsible for COVID-19 and other diseases that are transmitted *via* aerosols. And while Far UV-C sources will promote photochemical generation of ozone from molecular oxygen, the rates of ozone formation from these sources are modest, such that ozone concentrations in the vicinity of Far UV-C sources can be effectively controlled through conventional ventilation.

This combination of characteristics indicates that Far UV-C radiation may provide opportunities for new modes of application of UV-based disinfection systems. Specifically, it appears that it may be possible to implement Far UV-C radiation in systems that allow greater exposure of human tissues to the output from these UV devices than with conventional UV-C systems. This has the potential to fundamentally change how UV-C radiation can be applied for disinfection of air and surfaces.

Much of the knowledge base around Far UV-C radiation, its sources, and its application has emerged over the last 3–5 years. The goal of this article is to provide a comprehensive review of the current state-of-knowledge related to Far UV-C sources, their application for disinfection of air and surfaces, and the safety concerns related to Far UV-C radiation. Research needs related to Far UV-C sources and their applications are also presented.

UV radiation and far UV-C

UV radiation is defined as a band of electromagnetic radiation with wavelengths ranging from 100 to 400 nm (see Fig. 1). The UV spectrum has been divided into three major photobiological bands: UV-A (315–400 nm), UV-B (280–315 nm), and UV-C (100–280 nm); vacuum-UV (VUV, 100–200 nm) is defined as a sub-band of UV-C. For purposes of this review, we further sub-divide UV-C into the informally defined categories of conventional germicidal UV irradiation (UVGI, 250–280 nm) and Far UV-C (200–230 nm) radiation.¹

Sources of far UV-C radiation

UV-C disinfection processes depend on generation of radiation from artificial sources. Conventional UVGI systems are based on low-pressure mercury lamps, with primary and secondary emission lines at 253.7 and 184.9 nm, respectively; the latter emission line is normally eliminated by use of an envelope around the lamp that absorbs short wavelength radiation that is responsible for ozone generation. For Far UV-C radiation, the most common sources are barrier discharge excimer lamps (Sosnin et al., 2006) first developed in the 1980s (Tarasenko & Sosnin, 2012). In these devices, an electrical potential is applied across a sealed chamber containing a rare

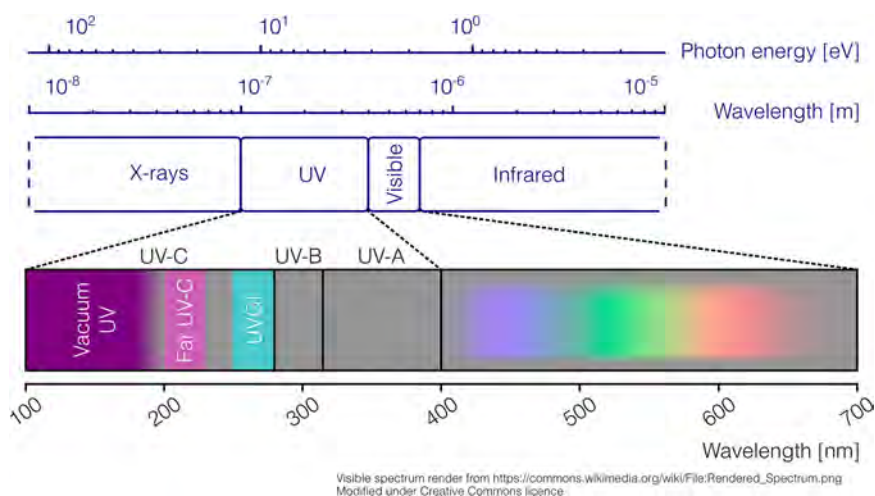


Figure 1. Electromagnetic spectrum and the position of ultraviolet radiation within it. Designations of the wavelength ranges that define UV-A, UV-B, and UV-C are shown, along with the sub-categories of UV-C (UVGI, Far UV-C, and VUV).

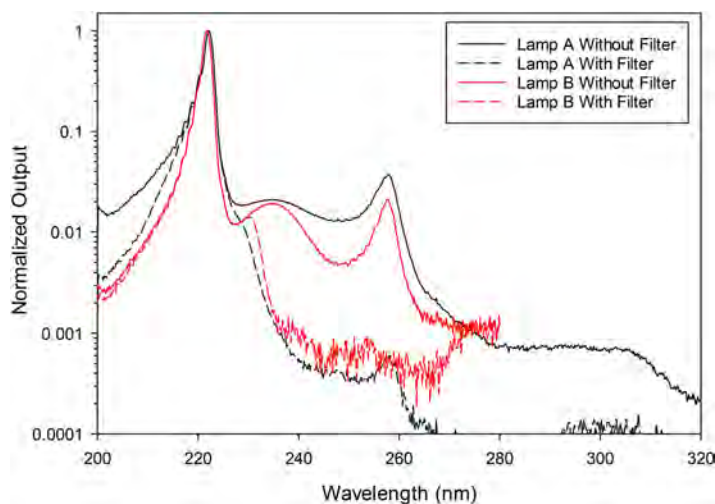


Figure 2. Emission spectra in the UV-C and UV-B ranges from commercially-available KrCl* lamps with and without optical filters. Normalized output presented on a log₁₀ scale. For both lamps, the spectra were measured independently and normalized to output at the wavelength corresponding to peak output (ca. 222 nm).

gas-halogen mixture, thereby exciting the gas into a plasma state. The resulting excited dimer (i.e., ‘excimer’) then undergoes an electronic transition to emit quasi-monochromatic radiation. The plasma may contain several excimers, leading to primary and secondary (weaker) emission peaks. To a limited degree, the contributions from different electronic transitions can be enhanced or suppressed by adjusting gas pressure and composition to ‘tune’ lamp output (Shuaibov et al., 2004).

In the context of Far UV-C radiation, most recent activity has focused on krypton-chloride excimer (KrCl*) lamps. Emission spectra vary somewhat depending on the lamp design, but KrCl* lamps typically exhibit a primary peak at ~222 nm with full-width-half-maximum ~4 nm; in addition there are also secondary emissions extending to 200 nm and below, as well as at wavelengths longer than the primary peak from other KrCl* and Cl₂* transitions (Sosnin et al., 2006),

extending to ~ 300 nm and above, with only trace emission at longer wavelengths, including in the UV-B range (Fig. 2). These secondary emissions can represent up to $\sim 15\%$ of the total power output of a typical unfiltered KrCl* lamp, as illustrated by their unfiltered output spectra (see Fig. 2).

The primary peak from a KrCl* lamp centered at 222 nm is well-suited to the applications that are discussed herein. Radiation at longer wavelengths can be problematic in terms of human eye and skin exposure risks, while shorter wavelengths can be problematic due to potential ozone generation. Consequently, most practical applications of KrCl* lamps include optical filters to reduce contributions of radiation from the secondary peaks (also illustrated in Fig. 2). A summary and comparison of basic characteristics of low-pressure mercury lamps and krypton chloride excimer lamps are presented in Table SI-1.

Other sources of Far UV-C radiation have been developed, including metallic vapor lamps (Zelikoff et al., 1952), optically-filtered medium-pressure mercury lamps (Beck et al., 2015), solid state emitters (e.g., Far UV-C LEDs), and lasers. To date, applications of these alternative Far UV-C sources have been limited to small-scale applications, often in research.

Inactivation by UV-C/far UV-C radiation

Mechanisms of inactivation

Wavelength and total UV exposure (commonly referred to as UV dose or fluence) are the two key parameters that control UV disinfection (Harm, 1980; Jagger, 1967). The germicidal efficacy of UV-C varies with wavelength and each microbe or virus being targeted has a unique response described by its germicidal action spectrum. Though germicidal action spectra among microbial and viral species are unique (Beck et al., 2015), a local peak in the 250–270 nm region is common, as this is where UV-C most effectively causes genomic damage resulting in pathogen inactivation. This fact, and the widespread availability of mercury vapor-based lamps (emitting predominantly at 254 nm), led to a focus on conventional mercury vapor lamps for UVGI systems.

Wavelengths in the Far UV-C region (200–230 nm) are highly efficient for pathogen inactivation due to the absorption of radiation by both nucleic acids and proteins (see Fig. SI-1); however, less is known about disinfection efficacy in the Far UV-C because sources operating at this region have only recently emerged as commercially viable. Far UV-C absorbance by nucleic acids and proteins can photochemically damage both biomolecule types, providing dual pathways to microorganism and virus inactivation.

While shorter wavelength Far UV-C photons can readily inactivate target pathogens, they can also be more highly absorbed by environmental (water, aerosols, and air) media, resulting in reduced photon flux and lower inactivation. For example, airborne viruses are often embedded within aerosol droplets, which themselves can contain proteins at relatively high concentrations. The presence of any absorbing compounds (e.g., proteins) can inhibit the ability of UV-C radiation, including radiation in the Far UV-C range, to penetrate aerosols. In quantitative terms, aerosol diameter and composition will control delivery of photons to aerosolized target pathogens (Barancheshme et al., 2021). The effects of absorbance by proteins and other constituents in aerosols are expected to be minimal due to the short optical pathlength, but improvement in understanding the effects of this behavior more quantitatively is an area for future research.

UV-C inactivation data

UV-C irradiation is effective for inactivation of microbial and viral pathogens in air, water, and on surfaces. Coronaviruses specifically are rapidly inactivated by UV-C radiation, as illustrated in Fig. 3. Only data from studies conducted employing accepted guidelines or best practice and

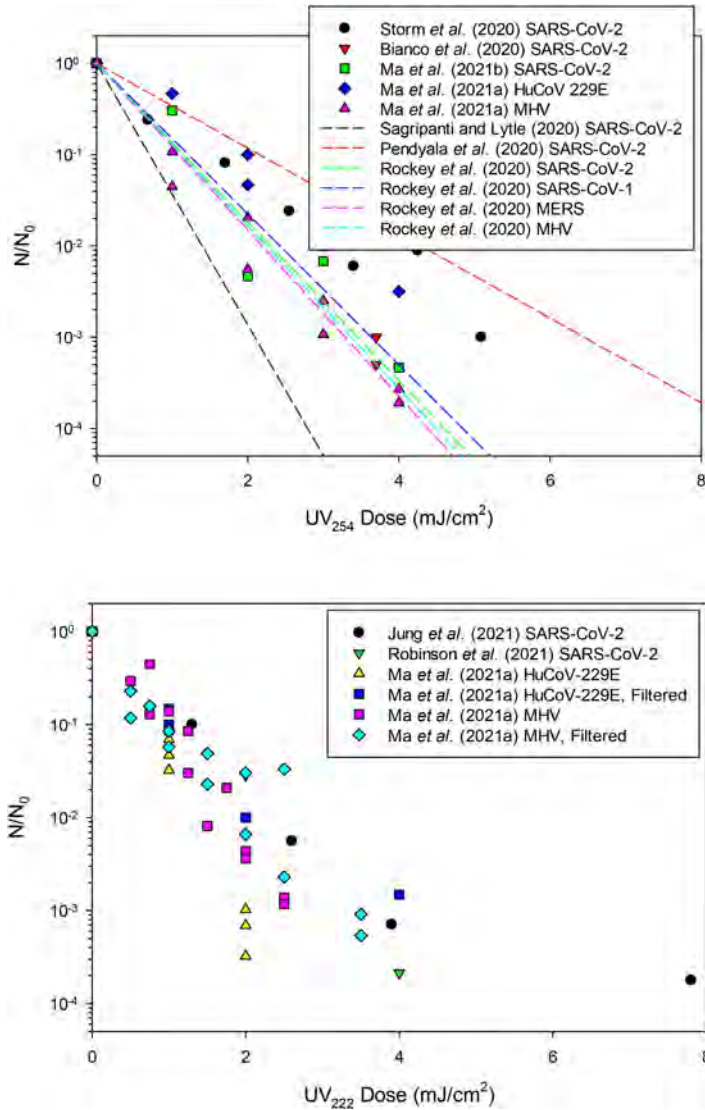


Figure 3. (Top) UV_{254} inactivation of coronaviruses, in aqueous suspension (Bianco et al., 2020; Ma, Gundy, et al., 2021; Ma, Linden, et al., 2021; Storm et al., 2020). Genomic model predictions of coronavirus responses are indicated by dashed lines (Pendyala et al., 2020; Rockey et al., 2020; Sagripanti & Lytle, 2020). (Bottom) UV_{222} inactivation of coronaviruses in aqueous suspension (Jung et al., 2021; Ma, Linden, et al., 2021; Robinson et al., 2021).

methods for measuring UV dose and for assessing viral inactivation were included in this graphical representation (Bolton & Linden, 2003). In aqueous (liquid) suspensions of viruses, high levels of inactivation are achieved with irradiation from a conventional UV_{254} lamps, which was also true for sources that emit at other UV-C wavelengths, including Far UV-C.

At 254 nm approximately 1 \log_{10} reduction of coronaviruses is achieved for each 2 mJ/cm^2 delivered UV-C fluence (dose). For comparison, other human pathogenic viruses, such as poliovirus and rotavirus require about 4–5 times that amount (i.e., 8–10 mJ/cm^2) for each \log_{10} unit reduction (Masjouidi et al., 2021).

UV_{222} irradiation is at least as effective as UV_{254} irradiation for inactivation of viruses, with approximately 1 \log_{10} reduction of coronaviruses achieved for each 1 mJ/cm^2 of delivered UV-C

Table 1. Summary of genetic properties of human viruses and bacteriophage described herein.

Virus	Genome Type	Enveloped or non-enveloped	Genome size (kilobases or kilobase pairs)	NCBI accession
SARS-CoV-2	ssRNA	Enveloped	29.8 kb	MN908947
SARS-CoV-1	ssRNA	Enveloped	29.7 kb	NC_004718
MERS	ssRNA	Enveloped	30.1 kb	NC_019843.3
MHV	ssRNA	Enveloped	31.3 kb	AY700211
HuCoV-229E	ssRNA	Enveloped	27.3 kb	NC_002645
HuCoV-OC43	ssRNA	Enveloped	30.7 kb	NC_006213
Influenza A (H1N1)	segmented ssRNA	Non-enveloped	13.5 kb	NC_002016-002023
Adenovirus (Type 2)	dsDNA	Non-enveloped	35.9 kb	AC_000007
Φ6 Bacteriophage	segmented dsRNA	Enveloped	13.4 kb	NC_003714-003716
T1 Bacteriophage	dsDNA	Non-enveloped	48.8 kb	NC_005833
T1UV Bacteriophage	dsDNA	Non-enveloped	(Assumed similar to T1)	n/a
Qβ Bacteriophage	ssRNA	Non-enveloped	4.2 kb	NC_001890
MS2 Bacteriophage	ssRNA	Non-enveloped	3.6 kb	NC_001417

Sequencing information can be found in <https://www.ncbi.nlm.nih.gov/>, using NCBI accession number.

fluence or less. In other words, irradiation at 222 nm provides roughly twice the rate of inactivation as observed at 254 nm.

Genome size and make-up are key factors governing the response of viruses to UV-C radiation (Lytle & Sagripanti, 2005; Pendyala et al., 2020; Rockey et al., 2020; Sagripanti & Lytle, 2020). In general, larger genomes provide more targets for photochemical damage; therefore, viruses and other pathogens with relatively large genomes tend to be inactivated relatively quickly. The type of genome (either single-stranded [ss], double-stranded [ds], RNA, or DNA) also influences the response of viruses to UV-C exposure. Coronaviruses have the largest known genomes among ss-RNA viruses; this is likely an important contributing factor to the facile inactivation of coronaviruses by UV-C exposure. Viruses with ds DNA genomes are often relatively resistant to UV-C exposure because the complementary nucleic acid strand can facilitate repair within its host (Boszko & Rainbow, 1999; Rodriguez et al., 2014; Shin et al., 2009). The presence of a viral envelope can influence the susceptibility of viruses to exposure to some physical agents, such as heat or shear forces. However, the presence of a viral envelope may not have any influence on the response of viruses to UV-C exposure. A summary of the genetic properties of the viruses and bacteriophage reported herein is presented in Table 1.

Inactivation models have recently been developed based on genomic properties of viruses for UV₂₅₄ irradiation (Pendyala et al., 2020; Rockey et al., 2020; Sagripanti & Lytle, 2020). These models yield predictions of viral inactivation at 254 nm that are similar to reported measurements; moreover, the predictions of these independently-developed models are consistent with each other. Currently, no models have been developed to characterize UV dose-response behavior for 222 nm UV irradiation. The inclusion of terms to address protein damage in Far UV-C inactivation (Beck et al., 2018) will complicate predictions that are based solely on genomic characteristics. Enhanced inactivation of viruses at Far UV-C wavelengths has been shown to be due to protein damage (Beck et al., 2018), as represented by studies on respiratory adenoviruses illustrated in Fig. SI-2 (Beck et al., 2014; Linden et al., 2007).

The kinetics of coronavirus inactivation by UV irradiation on surfaces or in aerosols appear to be at least as fast as those for the same virus in aqueous suspension, with greater than 1 log₁₀ reduction achieved for each 2 mJ/cm² delivered UV fluence (see Fig. SI-3). More generally, inactivation of viruses suspended in water or other aqueous media appears to provide an equivalent or slightly more conservative estimate of the intrinsic inactivation response that can be achieved on surfaces or in aerosols, based on these and other available UV inactivation data.

While these data suggest that UV inactivation of viruses on surfaces or in aerosols is expected to be as fast or faster than in aqueous suspension, there are other complicating factors.

Inactivation of pathogens (including viruses) in aerosols and on surfaces by UV-C irradiation is also influenced by the optical properties of the surrounding media, including absorbance, reflectance, and refraction. As a result, quantifying UV-C dose delivery to (viral) pathogens in aerosols and on surfaces can be challenging. Current research is expanding on these initial findings to include other surface types and conditions.

Validation and modeling

UV-C disinfection experimental protocols for pathogen inactivation in aqueous suspensions are well standardized to deliver a controllable, quantifiable, single-valued dose to a viral population *via* a (pseudo) collimated beam (Blatchley III, 1997; Bolton et al., 2015; Bolton & Linden, 2003). For airborne and surface-associated viruses, no such standard currently exists, although guidelines and laboratory devices have been proposed and developed (Welch et al., 2018).

Practical applications of UV-C radiation for disinfection will be influenced by both the intrinsic kinetics of inactivation and the distribution of UV doses delivered to the pathogen population. Well-defined methods have been developed for quantification of the dose distribution delivered by UV photoreactors that are used for disinfection of water. These methods, which now represent the industry standards for design and analysis of UV disinfection systems, generally involve integrated applications of computational fluid dynamics, fluence rate field models, and a model to describe the intrinsic kinetics of inactivation (Ahmed et al., 2018, 2019; Chiu et al., 1999; Ducoste, Linden, et al., 2005; Ducoste, Liu, et al., 2005; Imoberdorf et al., 2008; Lyn et al., 1999; Naunovic et al., 2008; Sozzi & Taghipour, 2006). Analogous methods have been applied for evaluation of UV-C systems that are used for disinfection of air (Buchan et al., 2020). Similar numerical models may be developed to simulate dynamic behavior of UV-C disinfection systems used to disinfect surfaces. Like all numerical models, validation based on physical measurements is required. Research in this area is likely to continue to evolve as interest and demand for UV-based disinfection systems grows.

Beyond these numerical models, it is also important that empirical (experiment-based) methods be developed and applied for testing and validation of UV-C systems that are used to disinfect air and surfaces. It is likely that these methods will be derived from the analogous methods that have been standardized for validation of UV disinfection systems that are applied in water treatment in the USA (Emerick & Tchobanoglous, 2012; EPA, 2006) and in western Europe (German & Standardization I. F., 2020a, 2020b; ÖNORM, 2003, 2020a, 2020b). These standardized validation protocols are based on the use of surrogate challenge microbes or viruses to quantify disinfection efficacy. Given the history and success of these applications, which are based on measurements of inactivation of nonpathogenic challenge agents, it is likely that testing and validation protocols for UV disinfection systems for air and water will adopt similar strategies.

Surrogates and indicators of UV inactivation of respiratory viruses

A critical need exists to develop standardized protocols for validation of disinfection efficacy among UV systems designed for disinfection of air and surfaces. These protocols will almost certainly be based on *surrogates* for airborne pathogens that do not require high levels of biosafety. A good surrogate will be nonpathogenic to humans, easy to culture and assay, no more sensitive to UV exposure than the target pathogen at the wavelength(s) emitted by the UV source of interest, and not exhibit post-irradiation repair. Ideally, this viral surrogate will also be from a similar pathogen class and share genetic and structural similarities, such as nucleic acid make-up and the presence/absence of an envelope. UV inactivation of select viral surrogates can represent UV inactivation of coronaviruses at either 254 or 222 nm, as illustrated in Fig. 4.

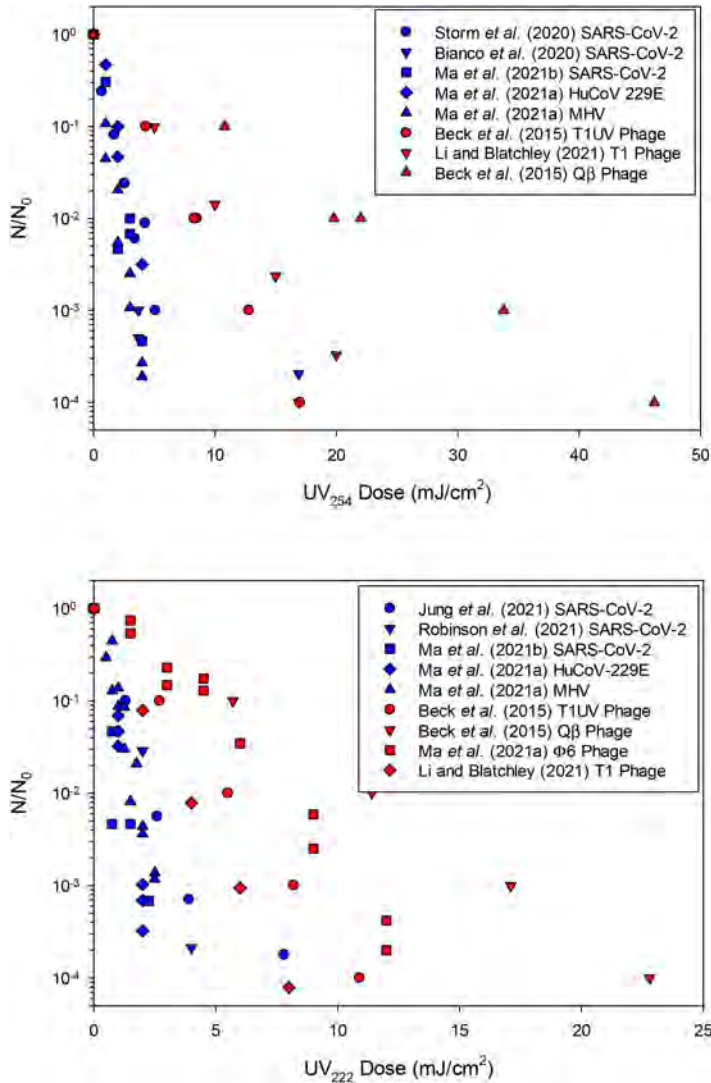


Figure 4. (Top) UV_{254} dose-response behavior of coronaviruses and phage that could serve as conservative surrogates (Beck *et al.*, 2015b; Bianco *et al.*, 2020; Li & Blatchley III, 2021; Ma, Linden, *et al.*, 2021; Storm *et al.*, 2020). (Bottom) UV_{222} dose-response behavior of coronaviruses and phage that could serve as conservative surrogates (Beck *et al.*, 2015; Ma, Linden, *et al.*, 2021; Robinson *et al.*, 2021). Coronavirus inactivation is indicated by blue symbols; potential phage surrogates are indicated by red symbols.

T1UV phage, T1 phage, and Q β phage all provide conservative representations of the rate of inactivation of coronaviruses at 254 nm. For 222 nm irradiation, T1UV, T1, and Φ 6 phage also provide conservative representations of the rate of inactivation of coronaviruses. MHV, a murine coronavirus with high genetic similarity to SARS-CoV-2, shows similar inactivation to it for both 254 and 222 nm irradiation. As noted in Table 1, T1 and T1UV phage are dsDNA viruses and are non-enveloped. Q β phage is a ssRNA virus, also non-enveloped. Φ 6 phage is an enveloped dsRNA virus. Data presented in Fig. 4 demonstrate that Φ 6 is only about 10% as sensitive to UV_{254} as the coronaviruses, whereas at 222 nm, Φ 6 represents a slightly conservative surrogate for the coronaviruses. As such, it appears that Φ 6 phage may represent a relevant surrogate for UV_{222} systems but not for UV_{254} systems. While the T1, T1UV, Q β , and Φ 6 phage are all easy to

propagate and assay using bacterial hosts, use of MHV requires mammalian cell culture infectivity assays which require more complex laboratory facilities and skilled virologists.

Conservatism is desirable in the selection of a viral surrogate, but overly conservative surrogate selections can provide misleading information about the performance of UV disinfection systems and may disqualify some technologies that can provide effective protection against airborne pathogens. This is not as simple a case as providing an extra degree of caution in the definition of standards for UV disinfection equipment. A minimum standard that is set too high will limit or negate the implementation of demonstrably effective disinfection apparatus without providing a viable alternative in their place; under such circumstances, a 'good enough' system that meets an established standard may not be implemented and result in an absence of intervention where an efficacious system could have been deployed. Therefore, it is generally desirable to select a surrogate that demonstrates UV dose–response behavior that is as close as possible to that of the target pathogen. Examples of phage that will meet this objective include T1UV at 254 nm and T1 at 222 nm.

For some applications, it may be desirable to quantify the performance of a UV disinfection system in a public setting using ambient airborne bacteria or viruses. This would involve the use of *indicator* viruses or bacteria routinely found in the public setting of interest. Desirable characteristics among indicators that may be used for this purpose include presence at sufficient concentration to allow quantification of disinfection efficacy, availability of a simple yet selective assay for viability or infectivity, lack of pathogenicity, and similarity in UV dose–response behavior to that of the target pathogen. These characteristics are similar to those of surrogates, described above. However, an important distinction is that tests with an indicator would involve ambient microbes or viruses in a public setting, whereas surrogates would be added to the air space in a controlled laboratory facility for purposes of testing.

The vast majority of UV dose–response data sets have been generated using aqueous suspensions of the target microbe or virus. However, there is evidence to indicate that air-exposed microbes or viruses may respond differently than those in aqueous suspension; more specifically, there is evidence to indicate that air-exposed microbes and viruses are inactivated faster than in aqueous suspension (Fletcher, 2004; McDevitt et al., 2007; Peccia et al., 2001; Xu et al., 2005; McDevitt et al., 2012; Lim & Blatchley, 2012). [Figure SI-4](#) illustrates the UV₂₂₂ dose–response behavior of three aerosolized viruses and an aerosolized bacterium.

The data presented in [Fig. SI-4](#) also indicate that *Staphylococcus aureus* may represent an appropriate, conservative surrogate for coronaviruses. In general, bacteria are easier to culture and assay than viruses as they do not require a host cell line or cell culture facilities to evaluate viability. However, many bacteria have access to repair pathways that do not exist for viruses, which could complicate the use of bacteria as a viral surrogate. Given the broad differences in the types and suitability of acceptable surrogates, a tailored approach to future validation protocols for these technologies should be taken across the range of possible Far UV-C applications.

In a recent study, measurements were made in a room-scale bioaerosol chamber of aerosolized airborne pathogen reduction by filtered 222 nm Far UV-C (Eadie et al., 2021). Airborne pathogen reduction, using *S. aureus* as a surrogate, was measured in a 4.2 × 3.4 × 2.3 m room containing a continuous source of aerosolized airborne pathogens, typical ventilation (3 air changes per hour [ACH]), and ceiling-mounted Far UV-C lamps. The experiments were performed at Far UV-C exposure conditions consistent with the current 222 nm threshold limit values (TLVs) for UV-C exposure and at exposure conditions consistent with proposed new TLVs (discussed below). Using lamps operated within the current TLV, a >92% reduction in live airborne pathogens was achieved after 15 min – equivalent to an additional 35 effective ACH (eACH) (see [Fig. 5](#)). Using exposure conditions consistent with the proposed new TLV (Slincy & Stuck, 2021) a 99.9% reduction in viable airborne pathogens was achieved after 5 min.

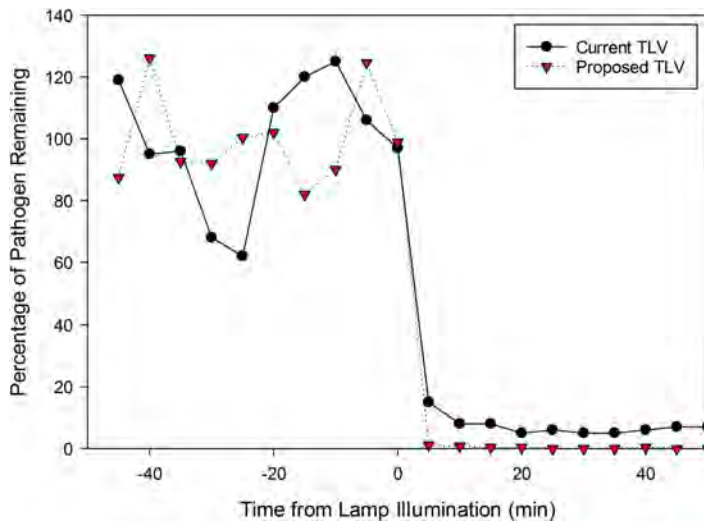


Figure 5. Percentage of viable aerosolized *S. aureus* remaining plotted as a function of time, measured from the time of lamp illumination ($t = 0$) in a bioaerosol chamber. Fresh air was introduced to the chamber at 3 ACH, in addition to continuous introduction of aerosolized *S. aureus*. Experiments were conducted using Far UV-C exposure that corresponded with the current and proposed TLVs for Far UV-C exposure, as of 2021. Data from Eadie et al. (2021).

Safety aspects of Far UV-C radiation exposure of human eyes and skin

The recent interest in applying Far UV-C to germicidal applications has stimulated investigations of health and safety of Far UV-C. Collectively, the studies demonstrate that exposures of both the eye and skin at wavelengths less than approximately 230 nm are substantially safer than longer UV-C wavelengths (Barnard et al., 2020; Buonanno et al., 2017, 2013, 2016, 2021; Cadet, 2020; Fukui et al., 2020; Hanamura et al., 2020; Hickerson et al., 2021; Kaidzu et al., 2019; Woods et al., 2015; Yamano et al., 2020). The experimental data are expected from the biophysical knowledge that Far UV-C radiation has much shorter penetration depths than longer wavelength UV-C radiation (Finlayson et al., 2021). UV-C radiation at wavelengths less than approximately 230 nm is strongly absorbed by all proteins (particularly through the peptide bond) as well as other biomolecules (Buonanno et al., 2013; Goldfarb & Saidel, 1951; Setlow, 1966) thus penetration into living tissue is very shallow, as shown in Fig. 6. These experimental findings have led to recommendations to revise Far UV-C guidelines to limit human exposure that can be applied to whole-room exposure in occupied settings (see below) (ACGIH, 2021; Sliney, 2013; Sliney & Stuck, 2021).

Skin

The greatest safety concern associated with germicidal UV-C applications has long been the potential for promotion of skin cancer (CIE, 2010; ISO, 2016; Sliney, 2013). This concern often originates without recognizing the action spectrum of photocarcinogenesis, which peaks with UV-B wavelengths (Fig. 6) (Forbes et al., 2020).

Epidemiological studies of solar-induced skin cancer clearly show the causal factor to be primarily attributable to UV-B radiation (Moan et al., 2015). Because so few people have been exposed to UV-C there have been no human epidemiological studies solely on UV-C exposure. Even so, it is clear that the outermost layer of skin (i.e., the human stratum corneum) strongly attenuates UV-C radiation such that very little UV-C radiation reaches the germinative, basal layer of the epidermis, where the DNA would have to be altered to potentially initiate skin cancer (CIE, 2010; Barnard et al., 2020; Cadet, 2020; Forbes et al., 2020). Since Far UV-C radiation is so

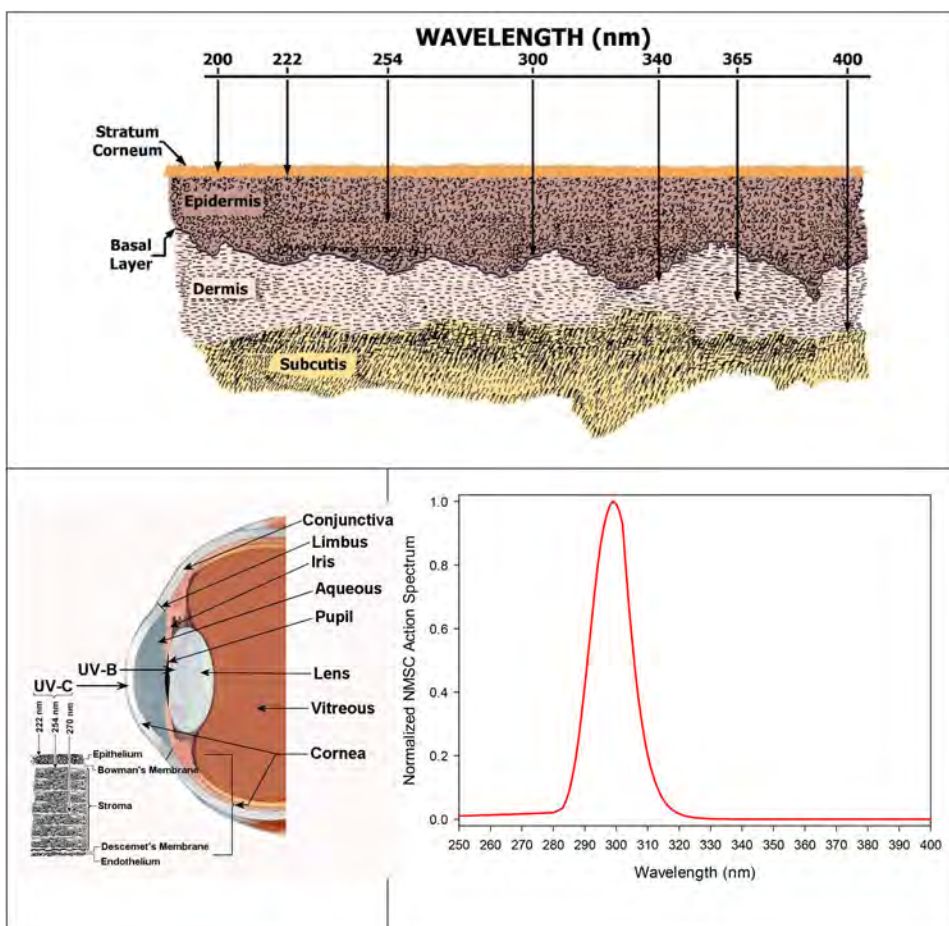


Figure 6. Effects of UV radiation on human tissues. (Top) Penetration of UV wavelengths into human skin. The arrows point to the estimated 90% absorption depths. UV-C wavelengths at 222 nm do not penetrate the stratum corneum; whereas, 254 nm penetrates into the upper epidermis. By contrast, UV-B wavelengths, such as 300 nm, penetrate to the germinative (basal) layer of the epidermis with sufficient energy to mutate DNA. The wavelengths of 340, 360, or 400 nm covering the UV-A penetrate deeply into the dermis but have lower photon energies that are far less damaging than 300 nm. (Lower Left) Penetration of UV wavelengths into the human eye. UV-C wavelengths at 222 nm hardly penetrate to the corneal epithelium; whereas, 254 nm penetrates well into the epithelium and into the stroma. The cornea blocks UV-C energy from reaching the lens (Oksala & Lehtinen, 1960) UV-B wavelengths, such as 300 nm, do penetrate to the lens, and oblique rays to the critically important germinative layer of the lens behind the iris and have sufficient energy to mutate DNA. UV-A wavelengths are strongly absorbed by fluorophores in the lens and protect the retina. (Lower right) International Standards Organization (ISO) standard action spectrum for non-melanoma skin cancer. This standard action spectrum was developed from extensive laboratory studies of skin cancer and measured spectral transmission of the stratum corneum and upper epidermis. Although it does not extend into the Far UV-C, it shows the significant risk of UV-B compared to UV-C. The risk for the far less penetrating Far UV-C would be still further reduced and vanishingly small (Data from ISO, 2016).

strongly absorbed in the stratum corneum, very little of this radiation can even reach the superficial layers of the epidermis, and essentially none can penetrate to the deeper basal layer, negating Far UV-C as a cancer risk (see Fig. 6).

All but one of the ten recently published experimental, peer-reviewed safety studies – both *in vitro* and *in vivo* – of the effects of Far UV-C radiation on human skin and hairless mouse skin showed no measurable negative impacts (Barnard et al., 2020; Buonanno et al., 2017, 2016, 2021; Cadet, 2020; Fukui et al., 2020; Hanamura et al., 2020; Hickerson et al., 2021; Yamano et al., 2020) despite including much larger doses than would be permitted in a human exposure scenario. The one published study (Woods et al., 2015) that did show evidence of skin

erythema used an unfiltered Far UV-C excimer lamp, i.e., with a biologically significant component of UV radiation at wavelengths >230 nm. This 2015 study was replicated by Fukui et al. (2020) using a spectrally-filtered 222 nm lamp (i.e., without the longer wavelengths) at similar or higher doses, showing no detectable erythema.

The *in-vivo* human skin erythema results support the laboratory findings by Buonanno et al. using an *ex-vivo* human skin model (EpiDerm) to assess photocarcinogenic effects. They found no significant increased occurrences of potentially-mutagenic cyclobutane-pyrimidine-dimer (CPD) DNA lesions after exposure to 125 mJ/cm^2 of unfiltered Far-UVC radiation. Only a slight increase of CPDs was detected at 500 mJ/cm^2 . Further evidence of a lack of photocarcinogenicity was shown by studies using hairless mice by Yamano et al. (2020) using two genotypes that were highly susceptible to photocarcinogenesis; they showed only a faint detection of CPDs only in the uppermost cells of the epidermis following exposure to a Far UV-C dose of 500 mJ/cm^2 . These findings further support *in-vivo* human skin studies (Hickerson et al., 2021).

It is important to note that the superficial, outer-most cells of the epidermis can no longer divide and are about to become the dead cells to form the outermost skin layer – the stratum corneum. All of these studies show an absence of, or non-consequential skin damage at very high exposures, above those typically required for disinfection thus supporting the use of germicidal Far UV-C exposure in occupied spaces.

Eye

Only a few studies of the effects of exposures to Far UV-C wavelengths on eye tissue exist (Oksala & Lehtinen, 1960; Pitts, 1974; Kaidzu et al., 2019; Kaidzu et al., 2021a, 2021b). Kaidzu et al. recently determined threshold photokeratitis in a rodent eye model at 24 hr post exposure employing slit-lamp bio-microscopy, surface mapping, and staining. They determined photokeratitis thresholds at four UV-C wavelengths (207, 222, 235, and 254 nm) and at one UV-B wavelength (311 nm). Thresholds at 207 and 222 nm were above 5000 and 15,000 mJ/cm^2 respectively, which are well above current safety guidelines. Kaidzu et al. (2019) and Kaidzu et al. (2021a, 2021b) also conducted a histological study of the cornea by measuring CPDs to detect DNA damage, which were analyzed for each wavelength and as a function of exposure dose. The depth of CPD biomarkers seen at 207 and 222 nm were limited to the upper superficial cells of the corneal epithelium, which are sloughed off in a day during a normal corneal epithelial life cycle. The germinative cells of the cornea are located in the limbus bordering the cornea and conjunctiva and are protected – as in the skin – from Far UV-C radiation by several cell layers (see Fig. 6). By contrast, at a longer UV-B wavelength, specifically 311 nm, CPDs were observed in all layers of the cornea including the corneal endothelium.

The corneal injury thresholds reported by Kaidzu et al. (2019) and Kaidzu et al. (2021a, 2021b) for Far UV-C radiation are significantly higher than those reported by Pitts (1974). The lower thresholds reported by Pitts can be explained by their use of wide-bandwidth, arc-monochromator exposures at 220, 240, and 250 nm, since the wide bandwidths (10 nm full-width, half-maximum, FWHM) led to an apparent action spectrum that was flattened – similar to an error in the 310-nm region (Chaney & Sliney, 2005). Since the Pitts data were applied during the development of the current UV exposure limits (Sliney et al., 1971; Sliney & Stuck, 2021) the lower UV-C limits now appear to be quite overly conservative, as explained further below.

Exposure limit guidelines

The current human exposure guidelines do not differ around the world. The most widely recognized limits are those of the American Conference of Governmental Industrial Hygienists (ACGIH) and the International Commission on Non-Ionizing Radiation Protection (ICNIRP).

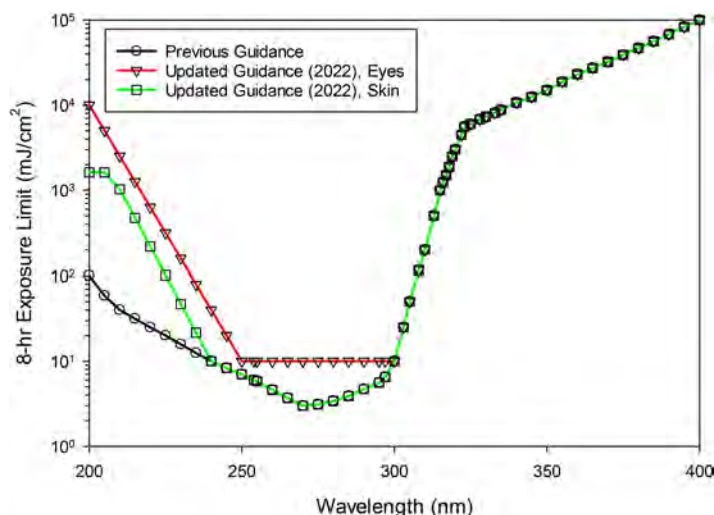


Figure 7. Comparison of 8-hr Threshold Limit Values (TLVs[®]) for UV-C radiation, based on relative spectral weighting values shown in Fig. SI-6. Data points indicate values as listed in the Guidance (ACGIH, 2022).

These had not changed for decades (ACGIH, 2021; ICNIRP, 2004), until recent guideline values were accepted (see discussion below). Both employed the same spectral weighting function, $S(\lambda)$, based upon threshold data for corneal and skin injury thresholds available in the 1970s. The UV-B data from monochromatic line spectra were given the highest importance (Sloney & Stuck, 2021). Figure SI-6 graphically summarizes these guideline values of $S(\lambda)$. Figure 7 illustrates the corresponding 8-h exposure limits.

The ACGIH issued a ‘Notice of Intended Change’ of UV-C TLVs in 2021. They proposed for the first time different limits for the eye and skin at wavelengths less than 300 nm as well as an increase in ocular limits at wavelengths below 250 nm (ACGIH, 2021). These revised guideline values were recently accepted by ACGIH (2022). The updated $S(\lambda)$ values for the skin and eye exposure are shown in Fig. SI-6 along with previous values. The corresponding exposure limits from the updated and previous values for $S(\lambda)$ are given in Fig. 7. The daily (based on an 8-hr exposure period), time-weighted exposure limits at 222 nm were increased from 23 mJ/cm² (for both skin and eyes) to 161 mJ/cm² for the eye and 479 mJ/cm² for the skin.

Risks for sensitive individuals for exposure to far UV-C radiation

The TLVs are guidelines to apply to nearly all individuals and are intended to be sufficiently conservative for the wide range of normal skin and eye sensitivities, including for individuals who are considered to have sensitive or photosensitive skin, or who have ‘dry eye’. Photosensitivity resulting from medications or other photosensitizers requires penetration well into the epidermis where photosensitizers would exist. Far UV-C exposure of the skin is considered much safer than longer UV-C wavelengths because of such shallow penetration depths; almost all incident photons are absorbed in the stratum corneum. The thickness of this layer does not vary significantly among individuals who may or may not possess ‘sensitive skin’ (Richters et al., 2017). This observation would argue against any individual differences because of skin diseases or by age, sex, or skin pigmentation (Lock-Andersen et al., 1997; Tagami, 2015). Correspondingly, the tear-layer thickness of the muco-aqueous tear layer or the lipid tear layer in healthy vs. even severe dry-eye patients show little difference (Segev et al., 2020). Therefore, the weight of evidence suggests that there are no significant subgroups of individuals who, by virtue of age, sex, race, health

conditions, or genetics, are systematically more sensitive than average to the effects of Far UV-C radiation.

Ozone generation by far UV-C lamps

Another safety-related concern related to Far UV-C-based applications is the potential to generate ozone. Ozone can be generated and decomposed by photochemical reactions; however, it should be noted that ozone may also be formed from corona discharges, which are associated with some Far UV-C sources. Moreover, the accumulation of ozone in ambient air will be governed not only by reactions that lead to formation and decay of ozone, but also air circulation and mixing in the vicinity of the Far UV-C source and room air exchange.

Reactions responsible for ozone formation and decay from far UV-C sources

Photochemical formation and destruction of ozone in the gas phase have been investigated extensively, largely because of the roles played by ozone in tropospheric and stratospheric chemistry, as well as with the use of vacuum UV (VUV) sources as ozone generators. Ozone (O_3) is generated by short wavelength UV radiation ($\lambda \leq 242 \text{ nm}$) or in electrical discharges (corona) when molecular oxygen (O_2) is present. Ozone can also be generated photochemically by a combination of ozone precursors (e.g., nitrogen oxides and hydrocarbons) at longer wavelengths UV ($290 \text{ nm} \leq \lambda \leq 400 \text{ nm}$), but this mechanism of ozone formation is unlikely to contribute significantly to ozone generation by Far UV-C sources.

Much of our current understanding of the potential for ozone formation from Far UV-C sources is based on studies of ozone formation and destruction in the stratosphere, which are initiated by photochemical reactions. The basic reactions that are responsible for photochemically-initiated formation and decomposition of ozone were first proposed by Sydney Chapman in 1930. The 'Chapman Cycle' comprises the following set of reactions (Chapman, 1930; Wayne, 1985). Note that 'M' refers to a non-reacting (chaperone) molecule:



Reactions 1 and 3 in this sequence are both photochemical. The rates of these reactions are governed by the rate at which UV photons in the relevant wavelength range are absorbed by the reactant molecules. In the case of reaction 1, the reactant is molecular oxygen (O_2), while for reaction 3 the reactant is ozone (O_3).

Net generation of ozone will depend on balance between the rates of ozone formation and decay; both processes are initiated photochemically. Ozone is a much stronger absorber of UV-C radiation than molecular oxygen on a per-molecule basis; however, the concentration of O_2 (in air) is many orders of magnitude larger than the concentration of O_3 . Consequently, the rate of reaction 1 is generally faster than the rate of reaction 3 with Far UV-C or VUV sources. For example, for a system operating with an air mixture at a total pressure of 1.0 atm with a temperature of 20°C and O_3 present near the regulatory limit for O_3 (0.1 ppm_v), with the ambient air being exposed to radiation at 222 nm (the peak wavelength from a KrCl* lamp), reaction 1 will proceed roughly 4.3 times faster than reaction 3. In a room where (essentially) no ozone is present (i.e., when a Far UV-C lamp is turned on), the ratio of the rates of ozone formation and

decay will be much larger. Therefore, the potential exists for generation of O₃ from Far UV-C sources.

Net production of O₃ by a Far UV-C source will depend on the fundamental chemistry described above, but also the conditions of application. Relevant conditions will include the output power and output spectrum of the Far UV-C source, as well as air circulation and mixing in the vicinity of the lamp.

Additionally, it should be noted that excimer lamps, depending on power and design, are driven by voltages in the 2–10 kV range, which are applied to the outside of the lamp. At these high voltages, there can be corona discharges on the exterior surface of the lamp. Since the discharge will happen in air, ozone generation by corona discharge can be an important contributor to ozone formation from a Far UV-C lamp and can be significantly higher than ozone generation by photochemical processes.

Ozone exposure limits

Ozone has been shown to affect the respiratory system as well as the cardiovascular and central nervous systems. Exposure limits for gas-phase ozone have been established by many governmental and non-governmental organizations that have responsibilities to ensure public health. [Table SI-2](#) provides a summary of exposure limits for O₃ that have been established by several of these organizations. In general, these limits call for gas-phase O₃ concentration to be maintained less than 0.05–0.1 ppm_v.

Ozone generation measurements

Two leading manufacturers of KrCl* lamps provided typical, measured ozone generation rates for their lamps. The lamps were operated at <12 W electrical power. The manufacturers reported significantly different generation rates of 70 µg/hr (7.7 µg O₃/W·h) and 12 µg/hr (1.1 µg O₃/W·hr). One manufacturer also reported data for a 70 W lamp of 12 mg/hr (170 µg O₃/W·hr).

It must be noted that the coaxial design of that lamp is quite different from the previously-mentioned low power lamps. The substantially higher ozone generation rate of this lamp is attributable to the contributions of corona discharges on the outside of the lamp, which led to much higher ozone generation than by just photochemical processes. It should also be noted that experiments show that ozone generation can be reduced by three times or more when optical filters are applied that absorb photons at wavelengths less than 200 nm.

It is also worth noting that the methods used to measure ozone generation by these lamps were different between the two manufacturers. The development of an industry standard for this measurement is needed to clarify the potential for ozone production in applications of Far UV-C sources.

Ozone generation in applications

Control of ozone exposure to humans and the environment will require that ozone generation rates from these lamps be quantified using a standardized method. Since the lamps will always be used in fixtures, it is the responsibility of the fixture manufacturer to provide data to customers about ozone emission from the fixture.

For rough estimates of the room ozone concentration the following formula can be used:

$$\text{Ozone concentration} = \frac{\text{Ozone generation rate} \times \text{time}}{\text{Room volume}} \quad (7)$$

Using one of the above-mentioned lamps (<12 W) as an example, the maximum ozone accumulation within a room of 1000 cubic feet (28.3 m³ – standard room size for UL867) over 24 hr will be 0.027 ppm_v; such an installation would very likely fall below the UL867 upper limit (Underwriters Laboratories, 2000) of 0.050 ppm_v, particularly when ‘real world’ conditions of air mixing and in/outflow are also considered. In practical applications of these devices, air circulation from a conventional HVAC system can be used to maintain the ambient ozone concentration well below the limits that are presented in Table SI-2. By extension, this indicates that practical applications of Far UV-C sources should be developed by considering air circulation and mixing that is imposed on indoor air space by the existing HVAC system.

Given the number of variables in lamp design, emission spectrum, lamp power, lamp duty cycle, room volume, air circulation, and air exchange rates, it is not possible to say whether a given Far UV-C installation presents an ozone risk without assessing its specifics. Ozone generation by current Far UV-C lamps must be discussed by fixture manufacturers and considered by those installing or managing these fixtures.

Conclusions

Conventional germicidal UV-C radiation has been demonstrated to be effective for inactivation of airborne pathogens. Far UV-C radiation appears to be at least as effective as conventional UV-C radiation for microbial and viral inactivation, and available evidence gives a strong indication that this portion of the spectrum can be effective at controlling airborne disease transmission.

Implementation of UV-C systems for disinfection of air must be conducted in a manner that balances the need to inactivate airborne pathogens with the risks of UV-C exposure to humans. In the case of conventional UV-C systems, based on low-pressure mercury lamps as the source of radiation, this balance requires that humans be shielded from exposure to the output from these lamps. This is commonly achieved by any of three approaches: removal of human presence from the UV radiation sources (including presence-detection interlocks), isolation of the UV sources from occupied spaces (including in-duct designs and louvered housings), and controlling exposure to within accepted safe levels (based on radiometric measurements and occupation residence times). The same approaches to control equally apply to air disinfection systems based on Far UV-C sources.

In contrast with conventional germicidal UV-C, the potential for damage to human eye and skin tissues is greatly diminished with Far UV-C radiation, largely because of the limited extent of penetration of Far UV-C radiation into these tissues. As a result, the design and implementation of currently available Far UV-C sources (e.g., KrCl* lamps) may allow greater exposure of humans to this radiation than is acceptable for sources of conventional germicidal UV-C radiation. Along with the demonstrated efficacy in microbial inactivation, this gives a reasonable operating window where safe and effective solutions can be developed.

Current Far UV-C sources present two potential pathways for ozone generation through photolysis and electrostatic ionization of molecular oxygen. However, their potential for ozone generation is modest, indicating that control of ambient ozone concentration in rooms where Far UV-C is implemented can be accomplished with conventional HVAC systems and well-established approaches to ventilation.

Taken together, these attributes suggest that air disinfection systems based on Far UV-C radiation have the potential to function as effective measures for reducing the likelihood of airborne disease transmission, including highly transmissible diseases such as influenza, the measles, the common cold, and COVID-19. As such, these devices appear to have characteristics that will allow them to play important roles in controlling the current pandemic, as well as future pandemics and epidemics involving airborne pathogens.

Note

1. The wavelength ranges listed above conform to the definitions provided by the International Commission on Illumination (CIE) (see <http://cie.co.at/eilvterm/17-21-008>). The International Union of Pure and Applied Chemistry (IUPAC) presents a slightly different set of wavelength ranges for these categories of UV radiation (see <https://goldbook.iupac.org/terms/view/UT07492>). Specifically, the IUPAC defines UV-A and UV-B in the same manner as CIE, but defines UV-C as radiation with wavelengths of 200–280 nm, while VUV is defined as radiation with wavelengths of 100–200 nm.

Acknowledgments

This manuscript was assembled by a Task Force that was convened by the International Ultraviolet Association (IUVA; <https://iuva.org/>). The charge to the Task Force was assembling a comprehensive summary of the current state-of-knowledge related to Far UV-C applications for disinfection of air.

Disclosure of interest statement

No potential conflict of interest was reported by the authors.

ORCID

Ernest R. Blatchley  <http://orcid.org/0000-0002-4561-8635>

References

- CIE. (2010). *UV-C photocarcinogenesis risks from germicidal lamps*. CIE
- ACGIH. (2021). *2021 TLVs and BEIs: Based on the documentation of the threshold limit values for chemical and physical agents & biological exposure indices*. ACGIH.
- ACGIH. (2022). *2022 TLVs and BEIs*. American Conference of Governmental Industrial Hygienists.
- Ahmed, Y. M., Jongewaard, M., Li, M. K., & Blatchley, E. R. III. (2018). Ray tracing for fluence rate simulations in ultraviolet photoreactors. *Environmental Science & Technology*, 52(8), 4738–4745. <https://doi.org/10.1021/acs.est.7b06250>
- Ahmed, Y. M., Ortiz, A. P., & Blatchley, I. I. I., E. R. (2019). Stochastic evaluation of disinfection performance in large-scale open-channel UV photoreactors. *Journal of Environmental Engineering*, 145(10), 04019071. [https://doi.org/10.1061/\(ASCE\)EE.1943-7870.0001562](https://doi.org/10.1061/(ASCE)EE.1943-7870.0001562)
- Barancheshme, F., Philiber, J., Noam-Amar, N., Gerchman, Y., & Barbeau, B. (2021). Assessment of saliva interference with UV-based disinfection technologies. *Journal of Photochemistry and Photobiology B: Biology*, 217, 112168. <https://doi.org/10.1016/j.jphotobiol.2021.112168>
- Barnard, I. R. M., Eadie, E., & Wood, K. (2020). Further evidence that far-UVC for disinfection is unlikely to cause erythema or pre-mutagenic DNA lesions in skin. *Photodermatology, Photoimmunology & Photomedicine*, 36(6), 476–477. <https://doi.org/10.1111/phpp.12580>
- Beck, S. E., Hull, N. M., Poepping, C., & Linden, K. G. (2018). Wavelength-dependent damage to adenoviral proteins across the germicidal UV spectrum. *Environmental Science & Technology*, 52(1), 223–229. <https://doi.org/10.1021/acs.est.7b04602>
- Beck, S. E., Rodriguez, R. A., Linden, K. G., Hargy, T. M., Larason, T. C., & Wright, H. B. (2014). Wavelength dependent UV inactivation and DNA damage of adenovirus as measured by cell culture infectivity and long range quantitative PCR. *Environmental Science & Technology*, 48(1), 591–598. <https://doi.org/10.1021/es403850b>
- Beck, S. E., Wright, H. B., Hargy, T. M., Larason, T. C., & Linden, K. G. (2015). Action spectra for validation of pathogen disinfection in medium-pressure ultraviolet (UV) systems. *Water Research*, 70, 27–37. [pii] <https://doi.org/10.1016/j.watres.2014.11.028>
- Bianco, A., Biasin, M., Pareschi, G., Cavalleri, A., Cavatorta, C., Fenizia, F., Galli, P., Lessio, L., Lualdi, M., Redaelli, E., Saulle, I., Trabattoni, D., Zanutta, A., & Clerici, M. (2020). UV-C Irradiation is highly effective in inactivating and inhibiting SARS-CoV-2 replication. *SSRN Electronic Journal*, 11, 6260. <https://doi.org/10.2139/ssrn.3620830>
- Blatchley, E. R. III. (1997). Numerical modelling of UV intensity: Application to collimated-beam reactors and continuous-flow systems. *Water Research*, 31(9), 2205–2218. [https://doi.org/10.1016/S0043-1354\(97\)82238-5](https://doi.org/10.1016/S0043-1354(97)82238-5)

- Bolton, J. R., Beck, S., & Linden, K. G. (2015). *Protocol for the determination of fluence (UV dose) using a low-pressure or low-pressure high-output UV lamp in bench-scale collimated beam ultraviolet experiments*. <https://iuva.org/resources/Resource%20Documents/Bolton-Protocol%20for%20the%20Determination%20of%20Fluence.pdf>
- Bolton, J. R., & Linden, K. G. (2003). Standardization of methods for fluence (UV dose) determination in bench-scale UV experiments. *Journal of Environmental Engineering*, 129(3), 209–215. [https://doi.org/10.1061/\(ASCE\)0733-9372\(2003\)129:3\(209\)](https://doi.org/10.1061/(ASCE)0733-9372(2003)129:3(209))
- Boszko, I. P., & Rainbow, A. J. (1999). Removal of UV photoproducts from an adenovirus-encoded reporter gene following infection of unirradiated and UV-irradiated human fibroblasts. *Somatic Cell and Molecular Genetics*, 25(5–6), 301–315. <https://doi.org/10.1023/a:1019916415806>
- Buchan, A. G., Yang, L., & Atkinson, K. D. (2020). Predicting airborne coronavirus inactivation by far-UVC in populated rooms using a high-fidelity coupled radiation-CFD model. *Scientific Reports*, 10(1), 19659. <https://doi.org/10.1038/s41598-020-76597-y>
- Buonanno, M., Ponnaiya, B., Welch, D., Stanislauskas, M., Randers-Pehrson, G., Smilenov, L., Lowy, F. D., Owens, D. M., & Brenner, D. J. (2017). Germicidal efficacy and mammalian skin safety of 222-nm UV light. *Radiation Research*, 187(4), 483–491. <https://doi.org/10.1667/RR0010CC.1>
- Buonanno, M., Randers-Pehrson, G., Bigelow, A. W., Trivedi, S., Lowy, F. D., Spotnitz, H. M., Hammer, S. M., & Brenner, D. J. (2013). 207-nm UV light - a promising tool for safe low-cost reduction of surgical site infections. I: in vitro studies. *PLoS One*, 8(10), e76968. [pii] <https://doi.org/10.1371/journal.pone.0076968>
- Buonanno, M., Stanislauskas, M., Ponnaiya, B., Bigelow, A. W., Randers-Pehrson, G., Xu, Y., Shuryak, I., Smilenov, L., Owens, D. M., & Brenner, D. J. (2016). 207-nm UV light-A promising tool for safe low-cost reduction of surgical site infections. II: In-vivo safety studies. *PLoS One*, 11(6), e0138418. [pii] <https://doi.org/10.1371/journal.pone.0138418>
- Buonanno, M., Welch, D., & Brenner, D. J. (2021). Exposure of human skin models to KrCl excimer lamps: The impact of optical filtering. *Photochemistry and Photobiology*, 97(3), 517–523. <https://doi.org/10.1111/php.13383>
- Cadet, J. (2020). Harmless effects of sterilizing 222-nm far-UV radiation on mouse skin and eye tissues. *Photochemistry and Photobiology*, 96(4), 949–950. <https://doi.org/10.1111/php.13294>
- Chaney, E. K., & Sliney, D. H. (2005). Re-evaluation of the ultraviolet hazard action spectrum-the impact of spectral bandwidth. *Health Physics*, 89(4), 322–332. <https://doi.org/10.1097/01.HP.0000164650.96261.9d>
- Chapman, S. (1930). A theory of upper-atmospheric ozone. *Memoirs of the Royal Meteorological Society*, 3(26), 103–125.
- Chiu, K., Lyn, D. A., Savoye, P., & Blatchley III, E. R. (1999). Integrated UV disinfection model based on particle tracking. *Journal of Environmental Engineering*, 125(1), 7–16. [https://doi.org/10.1061/\(ASCE\)0733-9372\(1999\)125:1\(7\)](https://doi.org/10.1061/(ASCE)0733-9372(1999)125:1(7))
- Ducoste, J., Linden, K., Rokjer, D., & Liu, D. (2005). Assessment of reduction equivalent fluence bias using computational fluid dynamics. *Environmental Engineering Science*, 22(5), 615–628. <https://doi.org/10.1089/ees.2005.22.615>
- Ducoste, J. J., Liu, D., & Linden, K. (2005). Alternative approaches to modeling fluence distribution and microbial inactivation in ultraviolet reactors: Lagrangian versus Eulerian. *Journal of Environmental Engineering*, 131(10), 1393–1403. [https://doi.org/10.1061/\(ASCE\)0733-9372\(2005\)131:10\(1393\)](https://doi.org/10.1061/(ASCE)0733-9372(2005)131:10(1393))
- Eadie, E., Hiwar, W., Fletcher, L., Emma, T. O'Mahoney, P., Buonanno, M., Welch, D., Adamson, C. S., Brenner, D. J., Noakes, C., & Wood, K. (2021). *Far-UVC efficiently inactivates an airborne pathogen in a room-sized chamber*. <https://assets.researchsquare.com/files/rs-908156/v1/a54f46e0-47eb-4424-942f-b162aa4970fe.pdf?c=1631889559>
- Emerick, R. W., & Tchobanoglous, G. (2012). *Ultraviolet disinfection guidelines for drinking water and water reuse*. NWRI.
- EPA. (2006). *Ultraviolet disinfection guidance manual for the final long term 2 enhanced surface water treatment rule* (EPA 815-R-06-007). EPA.
- Finlayson, L., Barnard, I. R. M., McMillan, L., Ibbotson, S. H., Brown, C. T. A., Eadie, E., & Wood, K. (2021). Depth penetration of light into skin as a function of wavelength from 200 nm - 1000 nm. *Photochemistry and Photobiology*, <https://doi.org/10.1111/php.13550>
- Fletcher, L. A. (2004). The influence of relative humidity on the UV susceptibility of airborne gram negative bacteria. *IUVA News*, 6(1), 12–19.
- Forbes, P. D., Cole, C. A., Forbes, P. D., & deGrujil, F. (2020). *Origins and evolution of photocarcinogenesis action spectra, including germicidal UVC*. <https://doi.org/10.1111/php.13371>
- Fukui, T., Niikura, T., Oda, T., Kumabe, Y., Ohashi, H., Sasaki, M., Igarashi, T., Kunisada, M., Yamano, N., Oe, K., Matsumoto, T., Matsushita, T., Hayashi, S., Nishigori, C., & Kuroda, R. (2020). Exploratory clinical trial on the safety and bactericidal effect of 222-nm ultraviolet C irradiation in healthy humans. *PLoS One*, 15(8), e0235948. [pii] <https://doi.org/10.1371/journal.pone.0235948>
- German, & Standardization, I. F. (2020a). *Devices for the disinfection of water using ultraviolet radiation Part 1: Devices equipped with UV low pressure lamps - Requirements and testing* (Vol. DIN 19294-1:2020). German, & Standardization, I. F.

- German, & Standardization, I. F. (2020b). *Devices for the disinfection of water using ultraviolet radiation Part 3: Reference radiometers for devices equipped with UV low pressure lamps -Requirements and testing* (Vol. DIN 19294-3:2020). German, & Standardization, I. F.
- Goldfarb, A. R., & Saidel, L. J. (1951). Ultraviolet absorption spectra of proteins. *Science*, *114*(2954), 156–157.
- Hanamura, N., Ohashi, H., Morimoto, Y., Igarashi, T., & Tabata, Y. (2020). Viability evaluation of layered cell sheets after ultraviolet light irradiation of 222 nm. *Regenerative Therapy*, *14*, 344–351. [pii] <https://doi.org/10.1016/j.reth.2020.04.002>
- Harm, W. (1980). *Biological effects of ultraviolet radiation*. Cambridge University Press.
- Hickerson, R. P., Conneely, M. J., Tsutsumi, S. K. H., Wood, K., Jackson, D. N., Ibbotson, S. H., & Eadie, E. (2021). Minimal, superficial DNA damage in human skin from filtered far-ultraviolet-C (UV-C). *British Journal of Dermatology*, *184*(6), 1197–1199. <https://doi.org/10.1111/bjd.19816>
- ICNIRP. (2004). Guidelines on limits of exposure to ultraviolet radiation of wavelengths between 180 nm and 400 nm (incoherent optical radiation). *Health Physics*, *87*(2), 171–186.
- Imoberdorf, G. E., Taghipour, F., & Mohseni, M. (2008). Radiation field modeling of multi-lamp, homogeneous photoreactors. *Journal of Photochemistry and Photobiology A: Chemistry*, *198*(2–3), 169–178. <https://doi.org/10.1016/j.jphotochem.2008.03.006>
- Jagger, J. (1967). *Introduction to research in ultra-violet photobiology*. Prentice-Hall.
- Jung, W. K., Park, K. T., Lyoo, K. S., Park, S. J., & Park, Y. H. (2021). Demonstration of antiviral activity of far-UVC microplasma lamp irradiation against SARS-CoV-2. *Clinical Laboratory*, *67*, 1955–1958. <https://doi.org/10.7754/Clin.Lab.2020.201140>
- Kaidzu, S., Sugihara, K., Sasaki, M., Nishiaki, A., Igarashi, T., & Tanito, M. (2019). Evaluation of acute corneal damage induced by 222-nm and 254-nm ultraviolet light in Sprague-Dawley rats. *Free Radical Research*, *53*(6), 611–617. <https://doi.org/10.1080/10715762.2019.1603378>
- Kaidzu, S., Sugihara, K., Sasaki, M., Nishiaki, A., Ohashi, H., Igarashi, T., & Tanito, M. (2021a). Re-evaluation of rat corneal damage by short-wavelength UV revealed extremely less hazardous property of Far-UV-C†. *Photochemistry and Photobiology*, *97*(3), 505–516. <https://doi.org/10.1111/php.13419>
- Kaidzu, S., Sugihara, K., Sasaki, M., Nishiaki, A., Ohashi, H., Igarashi, T., & Tanito, M. (2021b). Re-evaluation of rat corneal damage by short wavelength UV revealed extremely less hazardous property of 222 nm-UV-C. *Private Communication*.
- Li, X., & Blatchley, E. R. III. (2021). *UV dose-response behavior of phage*. Purdue University.
- Lim, S., & Blatchley, E. R. III. (2012). UV dose-response behavior of air-exposed microorganisms. *Journal of Environmental Engineering*, *138*(7), 780–785. [https://doi.org/10.1061/\(ASCE\)EE.1943-7870.0000535](https://doi.org/10.1061/(ASCE)EE.1943-7870.0000535)
- Linden, K. G., Thurston, J., Schaefer, R., & Malley, J. P. (2007). Enhanced UV inactivation of adenoviruses under polychromatic UV lamps. *Applied and Environmental Microbiology*, *73*(23), 7571–7574. <https://doi.org/10.1128/AEM.01587-07>
- Lock-Andersen, J., Therkildsen, P., Olivarius, F. F., Gniadecka, M., Dahlstrom, K., Poulsen, T., & Wulf, H.-C. (1997). Epidermal thickness, skin pigmentation and constitutive photosensitivity. *Photodermatology, Photoimmunology & Photomedicine*, *13*(4), 153–158. <https://doi.org/10.1111/j.1600-0781.1997.tb00220.x>
- Lyn, D. A., Chiu, K., & Blatchley III, E. R. (1999). Numerical modeling of flow and disinfection in UV disinfection channels. *Journal of Environmental Engineering*, *125*(1), 17–26. [https://doi.org/10.1061/\(ASCE\)0733-9372\(1999\)125:1\(17\)](https://doi.org/10.1061/(ASCE)0733-9372(1999)125:1(17))
- Lytle, C. D., & Sagripanti, J. L. (2005). Predicted inactivation of viruses of relevance to biodefense by solar radiation. *Journal of Virology*, *79*(22), 14244–14252. <https://doi.org/10.1128/jvi.79.22.14244-14252.2005>
- Ma, B., Gundy, P. M., Gerba, C. P., Sobsey, M. D., & Linden, K. G. (2021). UV inactivation of SARS-CoV-2 across the UVC spectrum: KrCl* excimer, mercury-vapor, and light-emitting-diode (LED) sources. *Applied and Environmental Microbiology*, *87*(22), e01532-21. <https://doi.org/10.1128/AEM.01532-21>
- Ma, B., Linden, Y. S., Gundy, P. M., Gerba, C. P., Sobsey, M. D., & Linden, K. G. (2021). Inactivation of coronaviruses and phage Phi6 from irradiation across UVC wavelengths. *Environmental Science & Technology Letters*, *8*(5), 425–430. <https://doi.org/10.1021/acs.estlett.1c00178>
- Masjoudi, M., Mohseni, M., & Bolton, J. R. (2021). Sensitivity of bacteria, protozoa, viruses, and other microorganisms to ultraviolet radiation. *Journal of Research of the National Institute of Standards and Technology*, *126*, 1–77. <https://doi.org/10.6028/jres.126.02>
- McDevitt, J. J., Lai, K. M., Rudnick, S. N., Houseman, E. A., First, M. W., & Milton, D. K. (2007). Characterization of UVC light sensitivity of vaccinia virus. *Applied and Environmental Microbiology*, *73*(18), 5760–5766. <https://doi.org/10.1128/AEM.00110-07>
- McDevitt, J. J., Rudnick, S. N., & Radonovich, L. J. (2012). Aerosol Susceptibility of Influenza Virus to UV-C Light. *Applied and Environmental Microbiology*, *78*(6), 1666–1669. <https://doi.org/10.1128/AEM.06960-11>
- Moan, J., Grigalavicius, M., Baturaitė, Z., Dahlback, A., & Juzeniene, A. (2015). The relationship between UV exposure and incidence of skin cancer. *Photodermatology, Photoimmunology & Photomedicine*, *31*(1), 26–35. <https://doi.org/10.1111/php.12139>

- Naunovic, Z., Lim, S., & Blatchley, I. I. I., E. R. (2008). Investigation of microbial inactivation efficiency of a UV disinfection system employing an excimer lamp. *Water Research*, 42(19), 4838–4846. <https://doi.org/10.1016/j.watres.2008.09.001>
- Oksala, A., & Lehtinen, A. (1960). Light transmission of the corneal epithelium examined with an emission spectrophotograph. *Acta Ophthalmologica*, 38, 371–376. <https://doi.org/10.1111/j.1755-3768.1960.tb00202.x>
- ÖNORM. (2003). *Plants for the disinfection of water using ultraviolet radiation—Requirements and testing—Part 2: Medium pressure mercury lamp plants*. ÖNORM.
- ÖNORM. (2020a). *Devices for the disinfection of water using ultraviolet radiation Part 1: Devices equipped with UV low pressure lamps - requirements and testing* (Vol. ÖNORM M 5873-1:2020). ÖNORM.
- ÖNORM. (2020b). *Devices for the disinfection of water using ultraviolet radiation Part 3: Reference radiometers for devices equipped with UV low pressure lamps -Requirements and testing* (Vol. ÖNORM M 5873-3:2020).
- Organization, I. S. (2016). Photocarcinogenesis action spectrum (non-melanoma skin cancers). *Standard ISO/CIE 28077:2016(E)*. ISO.
- Peccia, J., Werth, H. M., Miller, S., & Hernandez, M. (2001). Effects of relative humidity on the ultraviolet induced inactivation of airborne bacteria. *Aerosol Science and Technology*, 35(3), 728–740. <https://doi.org/10.1080/02786820152546770>
- Pendyala, B., Patras, A., Pokharel, B., & D'Souza, D. (2020). Genomic modeling as an approach to identify surrogates for use in experimental validation of SARS-CoV-2 and HuNoV inactivation by UV-C treatment. *Frontiers in Microbiology*, 11, 572331. <https://doi.org/10.3389/fmicb.2020.572331>
- Pitts, D. G. (1974). The human ultraviolet action spectrum. *American Journal of Optometry and Physiological Optics*, 51(12), 946–960.
- Reed, N. G. (2010). The history of ultraviolet germicidal irradiation for air disinfection. *Public Health Reports (Washington, DC: 1974)*, 125(1), 15–27. <https://doi.org/10.1177/003335491012500105>
- Richters, R. J. H., Falcone, D., Uzunbajakava, N. E., Varghese, B., Caspers, P. J., Puppels, G. J., van Erp, P. E. J., & van de Kerkhof, P. C. M. (2017). Sensitive skin: Assessment of the skin barrier using confocal Raman microspectroscopy. *Skin Pharmacology and Physiology*, 30(1), 1–12. [pii] <https://doi.org/10.1159/000452152>
- Robinson, R. T., Mahfooz, N., Rosas-Mejia, O., Liu, Y., & Hull, N. M. (2021). SARS-CoV-2 disinfection in aqueous solution by UV₂₂₂ from a krypton chlorine excilamp. *medRxiv* 32. <https://doi.org/10.1101/2021.02.19.21252101>
- Rockey, N. C., Henderson, J. B., Chin, K., Raskin, L., & Wigginton, K. R. (2020). *Predictive modeling of virus inactivation by UV*. bioRxiv. <https://www.biorxiv.org/content/10.1101/2020.10.27.355479v1>
- Rodriguez, R. A., Bounty, S., Beck, S., Chan, C., McGuire, C., & Linden, K. G. (2014). Photoreactivation of bacteriophages after UV disinfection: Role of genome structure and impacts of UV source. *Water Research*, 55, 143–149. <https://doi.org/10.1016/j.watres.2014.01.065>
- Sagripani, J. L., & Lytle, C. D. (2020). Estimated inactivation of coronaviruses by solar radiation with special reference to COVID-19. *Photochemistry and Photobiology*, 96(4), 731–737. <https://doi.org/10.1111/php.13293>
- Segev, F., Geffen, N., Galor, A., Cohen, Y., Gefen, R., Belkin, A., Arieli, Y., Epshtein, S., Oren, A., & Harris, A. (2020). Dynamic assessment of the tear film muco-aqueous and lipid layers using a novel tear film imager (TFI). *The British Journal of Ophthalmology*, 104(1), 136–141. [pii] <https://doi.org/10.1136/bjophthalmol-2018-313379>
- Setlow, J. (1966). The molecular basis of biological effects of ultraviolet radiation and photoreactivation. In M. Ebert & A. Howard (Eds.), *Current topics in radiation research* (Vol. II, pp. 195–248). North Holland Publishing Company.
- Shin, G. A., Lee, J. K., & Linden, K. G. (2009). Enhanced effectiveness of medium-pressure ultraviolet lamps on human adenovirus 2 and its possible mechanism. *Water Science and Technology: A Journal of the International Association on Water Pollution Research*, 60(4), 851–857. <https://doi.org/10.2166/wst.2009.414>
- Shuaibov, A. K., Shevera, I. V., & General, A. A. (2004). Low-pressure ultraviolet emitter utilizing chlorine and krypton chloride molecules. *High Temperature*, 42(6), 875–878. <https://doi.org/10.1007/s10740-005-0030-7>
- Sliney, D. (2013). Balancing the risk of eye irritation from UV-C with infection from bioaerosols. *Photochemistry and Photobiology*, 89(4), 770–776. <https://doi.org/10.1111/php.12093>
- Sliney, D. H., Bason, F. C., & Freasier, B. C. (1971). The merits of an envelope action spectrum for ultraviolet exposure criteria. *American Industrial Hygiene Association Journal*, 32(7), 415–431. [10.1080/0002889728506722](https://doi.org/10.1080/0002889728506722)
- Sliney, D. H., & Stuck, B. E. (2021). A need to revise human exposure limits for ultraviolet UV-C radiation. *Photochemistry and Photobiology*, 97(3), 485–492.
- Sosnin, E. A., Oppenländer, T., & Tarasenko, V. F. (2006). Applications of capacitive and barrier discharge excilamps in photochemistry. *Journal of Photochemistry and Photobiology C: Photochemistry Reviews*, 7(4), 145–163. <https://doi.org/10.1016/j.jphotochemrev.2006.12.002>
- Sozzi, D. A., & Taghipour, F. (2006). UV reactor performance modeling by Eulerian and Lagrangian methods. *Environmental Science & Technology*, 40(5), 1609–1615. <https://doi.org/10.1021/es051006x>

- Storm, N., McKay, L., Downs, S., Johnson, R., Birru, D., de Samber, M., Willaert, W., Cennini, G., & Griffiths, A. (2020). Rapid and complete inactivation of SARS-CoV-2 by ultraviolet-C irradiation. *Scientific Reports*, *10*, 22421.
- Tagami, H. (2015). Stratum corneum cell layers. In M. A. Farage (Ed.), *Textbook of aging skin*. Springer-Verlag.
- Tarasenko, V. F., & Sosnin, E. A. (2012). Barrier-discharge excilamps: History, operating principles, prospects. *Journal of Optical Technology* *79*(10), 653–658. <https://doi.org/10.1364/JOT.79.000653>
- Underwriters Laboratories, I. (2000). *UL standard for safety for electrostatic air cleaners* (Vol. UL 867, pp. 82). Underwriters Laboratories, I.
- Wayne, R. P. (1985). *Chemistry of atmospheres*. Clarendon Press.
- Welch, D., Buonanno, M., Grilj, V., Shuryak, I., Crickmore, C., Bigelow, A. W., Randers-Pehrson, G., Johnson, G. W., & Brenner, D. J. (2018). Far-UVC light: A new tool to control the spread of airborne-mediated microbial diseases. *Scientific Reports*, *8*(1), 2752. <https://doi.org/10.1038/s41598-018-21058-w>
- Wells, W. F., & Fair, G. M. (1935). Viability of *B. coli* exposed to ultraviolet radiation in air. *Science*, *82*(2125), 280–281. <https://doi.org/10.1126/science.82.2125.280>
- Woods, J. A., Evans, A., Forbes, P. D., Coates, P. J., Gardner, J., Valentine, R. M., Ibbotson, S. H., Ferguson, J., Fricker, C., & Moseley, H. (2015). The effect of 222-nm UVC phototesting on healthy volunteer skin: A pilot study. *Photodermatology, Photoimmunology & Photomedicine*, *31*(3), 159–166. <https://doi.org/10.1111/phpp.12156>
- Xu, P., Kujundzic, E., Peccia, J., Schafer, M. P., Moss, G., Hernandez, M., & Miller, S. L. (2005). Impact of environmental factors on efficacy of upper-room air ultraviolet germicidal irradiation for inactivating airborne mycobacteria. *Environmental Science & Technology*, *39*(24), 9656–9664. <https://doi.org/10.1021/es0504892>
- Yamano, N., Kunisada, M., Kaidzu, S., Sugihara, K., Nishiaki-Sawada, A., Ohashi, H., Yoshioka, A., Igarashi, T., Ohira, A., Tanito, M., & Nishigori, C. (2020). Long-term effects of 222-nm ultraviolet radiation C sterilizing lamps on mice susceptible to ultraviolet radiation. *Photochemistry and Photobiology*, *96*(4), 853–862. <https://doi.org/10.1111/php.13269>
- Zelikoff, M., Wyckoff, P. H., Aschenbrand, L. M., & Loomis, R. S. (1952). Electrodeless discharge lamps containing metallic vapors. *Journal of the Optical Society of America*, *42*(11), 818–819. <https://doi.org/10.1364/JOSA.42.000818>